BIOCHEMISTRY
including biophysical chemistry & molecular biology

Article

pubs.acs.org/biochemistry

Design and Characterization of Stabilized Derivatives of Human CD4D12 and CD4D1

Piyali Saha,[†] Bipasha Barua,[†] Sanchari Bhattacharyya,[†] M. M. Balamurali,[†] William R. Schief,*[,‡] David Baker,[‡] and Raghavan Varadarajan*[,†]

[†]Molecular Biophysics Unit, Indian Institute of Science, Bangalore 560 012, India

[‡]Department of Biochemistry, University of Washington, Seattle, Washington 98105, United States

Supporting Information

ABSTRACT: CD4 is present on the surface of T-lymphocytes and is the primary cellular receptor for HIV-1. CD4 consists of a cytoplasmic tail, one transmembrane region, and four extracellular domains, D1−D4. A construct consisting of the first two domains of CD4 (CD4D12) is folded and binds gp120 with similar affinity as soluble 4-domain CD4 (sCD4). However, the first domain alone (CD4D1) was previously shown to be largely unfolded and had 3-fold weaker affinity for gp120 when compared to sCD4 [Sharma, D.; et al. (2005) *Biochemistry 44*, 16192−16202]. We now report the design and characterization of three single-site mutants of CD4D12 (G6A, L51I, and V86L) and one multisite mutant of CD4D1 (G6A/L51I/L5K/F98T). G6A, L51I, and V86L are cavity-filling mutations while L5K and F98T are surface mutations which were introduced to minimize the aggregation of CD4D1 upon removal of the second domain. Two mutations, G6A and V86L in CD4D12 increased the stability and yield of the protein relative to the wild-type protein. The mutant CD4D1 (CD4D1a) with the 4 mutations was folded and more stable compared to the original CD4D1, but both bound gp120 with comparable affinity. In *in vitro* neutralization assays, both CD4D1a and G6A-CD4D12 were able to neutralize diverse HIV-1 viruses with similar IC_{50}s as 4-domain CD4. These stabilized derivatives of human CD4 can be useful starting points for the design of other more complex viral entry inhibitors.

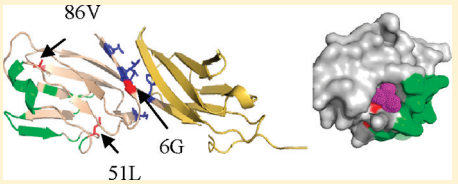

The HIV-1 envelope glycoprotein (env) consists of a trimer of dimers of two subunits, gp120 and gp41. These subunits are involved in receptor binding and fusion, respectively. The binding of HIV-1 gp120 to CD4, its primary cellular receptor on the surface of T-lymphocytes, is the first step in the entry of the virus into target cells.[1] CD4 is a 55 kDa glycoprotein that consists of four extracellular domains, D1−D4 (residues 1−371), one transmembrane domain (residues 372−395), and a cytoplasmic tail (residues 396−433) and is an important component of the immune system. It is expressed on T-lymphocytes as well as various other cells of the immune system. CD4 binds to gp120 with high affinity,[2] and the interaction takes place through its two N-terminal extracellular domains, D1 and D2, out of which only regions of domain1 (residues 25−85) make direct contact with gp120.[3] This interaction leads to a conformational change in gp120, resulting in exposure of previously hidden epitopes known as CD4-induced epitopes ($CD4_i$). The conformational change allows subsequent binding of gp120 to its cellular coreceptors CCR5 or CXCR4. Since virtually all strains of HIV-1 use the same receptor for viral entry, CD4 binding regions of gp120 are highly conserved among different clades of HIV-1, thus providing an ideal target for viral entry inhibition and broad neutralization activity. Recombinant, soluble four-domain CD4 (rsCD4) as well as two-domain CD4 (CD4D12) has been shown to bind to gp120 with high affinity and inhibit viral infection *in vitro*.[3−7] However, rsCD4 does not block infection of primary viral isolates *in vivo*.[8] This could be due to the short serum half-life of rsCD4 (∼30 min)[9] as well as the lower affinity of CD4 for trimeric env on the surface of primary isolates. Residues on gp120 that contact CD4 are relatively conserved, and monomeric gp120 from primary, hard to neutralize viruses has similar affinity to CD4 as gp120 from T-cell line adapted, easily neutralized viruses. Hence, it is likely that the higher IC_{50}s for soluble CD4 inhibition of primary viruses are because of the lower accessibility of the CD4 binding site on the trimeric envelope spike. More recently, it was reported that stabilization of a CD4D12−gp120 complex through interchain disulfide exchange led to an increase in the efficacy of viral entry inhibition.[10]

Previous studies have described the design and characterization of immunogens consisting of single-chain derivatives of gp120 linked to the first two domains of human CD4 (gp120−CD4D12) that elicited a broadly neutralizing immune response.[11,12] However, this broad neutralization was found to be exclusively due to anti-CD4 antibodies.[12] Therefore, it was postulated that construction of a minimized CD4 construct might help in reducing the immune response to CD4 in single-chain analogues. In a subsequent study, the design and characterization of several bacterially expressed and truncated derivatives of soluble CD4 (sCD4) protein were carried out.

Received: June 6, 2011
Revised: August 4, 2011
Published: August 9, 2011

These include CD4D12 corresponding to the two N-terminal extracellular domains (D1 and D2) of human CD4 (consisting of amino acids 1−183) and CD4D1 corresponding to the N-terminal domain, D1 of human CD4 (amino acids 1−99) with a few designed mutations at the D1:D2 interface.[13] CD4D12 bound to gp120 with similar affinity as full-length four-domain soluble CD4. However, CD4D1 bound with around a 3-fold reduction in affinity (K_D = 40 nM). This was possibly due to the fact that the designed CD4D1 is largely unfolded. Therefore, we hypothesized that the design of improved CD4D1 and CD4D12 constructs with increased stability might result in stronger binding with gp120 (for CD4D1) and increased bioavailability, hence leading to an improvement in viral entry inhibition *in vivo*. Steric restrictions in the trimeric envelope spike may be responsible for the relatively high IC_{50} values for soluble 4-domain and 2-domain CD4 for primary isolates observed previously.[8,14] Hence, it would be interesting to measure the IC_{50} for these isolates with a well-folded version of the smaller CD4D1 molecule, which might face fewer steric restrictions.

Burial of hydrophobic residues and high packing density in protein interiors make important contributions to protein stability. Hydrophobic cores of proteins have packing densities comparable to crystals of small organic molecules,[15,16] though a few cavities remain in the core of proteins. Several studies on cavity creating mutations have shown that these lead to loss in van der Waals contacts and decreased stability.[17−21] Attempts have therefore been made to stabilize proteins through cavity filling mutations. Previous attempts to increase the stability of T4 lysozyme by filling interior cavities failed due to unfavorable steric interactions[22] that resulted from the mutations. In the case of hen lysozyme (HEL), although cavity filling mutations have stabilized the enzyme, they have restricted the internal motion of the molecule, resulting in an increase in temperature for optimal enzymatic activity.[23,24] Cavity filling mutations in the hydrophobic core of the neutral protease of *Bacillus stearothermophilus* resulted in marginal stability of the molecule.[25] On the other hand, for RNase HI and c-myb, cavity filling mutations increased the stability of the molecule.[26−29] In the case of the metastable protein α1-antitrypsin, the conformational stability of the molecule increased linearly with increasing volume of the side chains of cavity filling mutations but led to decreasing serine protease inhibitor activity of the molecule.[30,31] The challenge in such studies is to introduce mutations without accompanying steric clashes or conformational strain.

In this study, we report the design and characterization of three single site cavity filling mutants of CD4D12 (G6A, L51I, and V86L) and one multisite mutant of CD4D1 (G6A/V86L/L5K/F98T). These mutations were based on predictions made by the ROSETTADESIGN algorithm[32] as well as the MC_CAVITY program[33] and were intended to increase protein stability. Stabilized and well-folded versions of CD4D12 and CD4D1 could be obtained, and both showed neutralization activity against a variety of HIV-1 strains with IC_{50} values ranging from 0.13 to 50 μg/mL. However, decreasing the size of the molecule from CD4D12 to CD4D1 did not substantially improve the IC_{50}.

EXPERIMENTAL PROCEDURES

Construct Descriptions. Wild-type CD4D12 (wt-CD4D12) refers to the first two N-terminal domains D1 and D2 (amino acids 1−183) of human CD4 (hCD4). As mentioned earlier,[13] according to the SCOP definition,[34] domain D1 corresponds to residues 1−97 of CD4; however, residues 98 and 99 interact with several residues within 1−97. In the present work, D1 refers to amino acids 1−99 and D2 refers to amino acids 100−183 of hCD4. CD4D1 (amino acids 1−99) is an engineered version of D1 with additional mutations described previously.[13] CD4D1a is the redesigned version of CD4D1 described in the present work.

ROSETTADESIGN and MC_CAVITY Calculation. Modeling of the mutations in CD4D12 and CD4D1 and associated energy calculations were done using the program ROSETTADESIGN (version 2.3.0).[32] The version of ROSETTADESIGN used (Rosetta_SmallRadii)[35] had the atomic radii scaled by 0.95 relative to standard CHARMM 19 radii. For cavity filling mutations the protein backbone was allowed to move, but in the case of mutations at the D1:D2 interface, the protein backbone remained fixed. For the movable backbone module the stereochemical parameters of the original PDB file were idealized before use. In the movable backbone module, the following command was used: rosetta.gcc -s pdbfilename -design -mvbb -paths pathsfilename -resfile resfilename -ex1 -ex2 -ex3 -ex4 -nstruct 5 -pdbout pdbprefixname. In the fixed backbone module the following command was used: rosetta.gcc -s pdbfilename -design -fixbb -paths pathsfilename -resfile resfilename -ex1 -ex2 -ex3 -ex4 -nstruct 5 -pdbout pdbprefixname. To detect cavities inside the protein molecule, the program MC_CAVITY was used.[33]

Construction and Expression of CD4D12 Constructs and CD4D1a. An *E. coli* codon-optimized version of the CD4D12 gene was synthesized and cloned into the pET28a(+) vector (Novagen) between the *NdeI* and *XhoI* sites and contained an N-terminal His tag. Three mutations were introduced individually in wt-CD4D12, namely G6A, L51I, and V86L. DNA encoding CD4D1 containing the mutations L5K, G6A, V86L, and F98T (referred to as CD4D1a) using overlap PCR was generated from CD4D12. The CD4D1a overlap product was then cloned into the pET28a(+) vector by restriction digestion and ligation of the 339 bp fragment obtained by overlap PCR. The rationale for these choices of mutation is described in a different section. *E. coli* strain BL21(DE3) cells transformed with the pET28a(+) plasmids were grown in 1 L of Luria-Broth (LB) at 37 °C until an OD of 0.6. Cells were then induced with 1 mM IPTG (isopropyl-β-thiogalactopyranoside) and grown for another 6 h at 37 °C for CD4D12 constructs and overnight at 30 °C for CD4D1 constructs. Cells were harvested at 3500*g* and resuspended in 30 mL of phosphate buffered saline (PBS), pH 7.4. The cell suspension was lysed by sonication on ice and centrifuged at 15000*g*. The supernatant was discarded, and the pellet was washed in 30 mL of 0.2% Triton X-100, PBS (pH 7.4) and subjected to centrifugation at 15000*g*. The pellet was solubilized in 25 mL of 8 M guanidine hydrochloride (GdnCl) in PBS (pH 7.4) overnight at room temperature. The solution was centrifuged at 15000*g* for 30 min. The supernatant was bound to 5 mL Ni-NTA beads (GE Healthcare) and washed with 30 mL of 50 mM imidazole containing 8 M guanidine hydrochloride in PBS. Denatured protein was eluted with 8 M GdnCl in PBS containing 500 mM imidazole at room temperature.

The first four eluted fractions (5 mL each) were pooled together and dialyzed extensively against PBS (pH 7.4) and 1

mM EDTA to remove the denaturant. Protein was ~90% pure as assessed by SDS-PAGE. The dialyzed protein was concentrated to a final concentration of 0.5 mg/mL and flash-frozen in liquid nitrogen and stored in aliquots at −70 °C. The average yield for wtCD4D12 and V86L-CD4D12 was 20 mg/L of culture; for G6A-CD4D12 it was 25 mg/L of culture, and for CD4D1a it was 10 mg/L of culture. The yield was determined by densitometry analysis from SDS-PAGE using standard proteins of known concentrations. The concentrations of the proteins were also estimated by absorbance at 280 nm using extinction coefficients of 18 240 and 12 615 M^{-1} cm^{-1} calculated from the amino acid sequence[36] of CD4D12 and CD4D1a, respectively.

Gel Filtration Analysis of wt-CD4D12 and CD4D1a. Approximately 50 μg of each protein was analyzed by gel filtration chromatography in PBS buffer at room temperature on a Superdex-75 analytical gel filtration column. A standard curve of the elution volume versus the log of the molecular weight was generated using albumin (67 kDa), ovalbumin (43 kDa), carbonic anhydrase (29 kDa), and ribonuclease A (13.7 kDa) as molecular weight markers.

Surface Plasmon Resonance (SPR) Experiments. All SPR experiments were performed with a Biacore 2000 (Biacore, Uppsala, Sweden) optical biosensor at 25 °C. 1000 resonance units (RU) of JRFL gp120 was attached by standard amine coupling to the surface of a research grade CM5 chip. A sensor surface (without gp120 or any antibody) that has been activated and deactivated served as a negative control for each binding interaction. Various CD4 derivatives were passed over each sensor surface in a running buffer of PBS, pH 7.4, containing 0.01% P20 surfactant. Analyte concentrations ranged from 25 to 200 nM for 4-domain CD4 and CD4D1 and from 25 to 150 nM for CD4D1a. Both binding and dissociation were measured for 100 s, respectively, at a flow rate of 30 μL/min. In all cases, the sensor surface was regenerated between binding reactions by one to two washes with 4 M $MgCl_2$ for 30 s at 30 μL/min. Each binding curve was corrected for nonspecific binding by subtraction of the signal obtained from the negative-control flow cell. The kinetic parameters were obtained by fitting the data to the simple 1:1 Langmuir interaction model by using BIA EVALUATION 3.1 software.

Far-UV Circular Dichroism (CD) and Fluorescence Spectroscopy. Circular dichroism (CD) spectra were recorded on a Jasco J-715C spectropolarimeter flushed with nitrogen gas. The concentration of protein sample was 15 μM, and buffer used was PBS, pH 7.4. Measurements were recorded in a 1 mm path length quartz cuvette with a scan rate of 50 nm/min, a response time of 4 s, and a spectral bandwidth of 2 nm. Each spectrum was an average of three scans. Mean residue ellipticities (MRE) were calculated as described previously.[12] Buffer spectra were also acquired under similar conditions and subtracted from protein spectra, before analysis. Thermal denaturation of the proteins were studied by measuring the CD signal at 222 nm from 20 to 95 °C in PBS (pH 7.4) buffer. Data were fit to a two-state thermal unfolding model as described previously.[37] The protein concentration and scan rate were 15 μM and 1 °C/min, respectively.

All fluorescence spectra were recorded at 25 °C on a SPEX Fluoromax3 spectrofluorimeter. For intrinsic fluorescence measurements, the protein concentration used was 2 μM. The excitation was at 280 nm, and emission was recorded from 300 to 400 nm. The excitation and emission slit widths were 3 and 5 nm, respectively. All fluorescence experiments were carried out in PBS at pH 7.4. For chemical denaturant induced unfolding studies of CD4D12 constructs and CD4D1a, 2 μM proteins were incubated in increasing concentrations of urea in PBS overnight at 25 °C and intrinsic fluorescence was measured at 350 and 365 nm for CD4D12 and CD4D1 proteins, respectively.

Proteolytic Digestion of wt-CD4D12, G6A-CD4D12, V86L-CD4D12, and CD4D1a. Proteolytic digestion of the above listed proteins and reduced carboxymethylated RNaseA (rcam-RNaseA) was carried out using trypsin at a protease/substrate molar ratio of 1:500. A total of 100 μg of protein was digested in 200 μL of digestion buffer (final concentration 50 mM HEPES, pH 8.0, 2 mM $CaCl_2$) at 37 and at 20 °C. At various times, 20 μL of sample was removed and trypsin was deactivated with 5 μL of 0.5% formic acid. 5 μL of SDS-PAGE gel-loading buffer (final concentration 50 mM Tris-HCl at pH 6.8 containing 2.0% SDS, 0.1% bromophenol blue, and 5% β-mercaptoethanol) was added; samples were boiled for 10 min and stored at −20 °C until use. Samples collected at different time points were subjected to analysis using 12% SDS-PAGE for CD4D12 constructs and 15% SDS-PAGE for CD4D1a followed by staining with Coomassie Brilliant Blue R250.

Serum Stability Check. To check the stability of the protein in serum, 30 μg of His-tagged CD4D1a (in 100 μL) was incubated in 100 μL of serum at 37 °C in the presence of 20 μL of Ni-NTA beads, and 40 μL aliquots were removed from the reaction mixture at different time points. For every time point, the beads were spun down, and both the supernatant and beads were subjected to 15% SDS-PAGE analysis.

Neutralization Assays. G6A-CD4D12 and CD4D1a were sent to Monogram Biosciences, Inc., for neutralization assays against clade B HIV-1 viruses (SF162, BAL, JRCSF, NL4-3) and clade C HIV-1 virus 98IN022. The assay used measures neutralization of HIV as a function of reductions in luciferase reporter gene expression after a single round of infection in U87 cells essentially as described previously.[38,39] Briefly, virus stocks are made by transfecting an envelope expression plasmid and a second plasmid that expresses the entire HIV-1 genome (except envelope) as well as an integrated reporter gene for firefly luciferase. Pseudovirions are treated with 3-fold serial dilutions of CD4 analogues, starting from 100 μg/mL for CD4D1a and 200 μg/mL for G6A-CD4D12 and subsequently incubated with U87 cells (engineered to express CD4 and CCR5/CXCR4). After 72 h, cells are washed and lysed, and the amount of luciferase produced is quantitated by adding the luciferin substrate. The degree of infection is directly proportional to the amount of RLUs measured. aMLV Env-expressing pseudo virions were used as negative controls. The IC_{50} is the concentration of CD4 inhibitor at which infection is reduced by 50%.

RESULTS AND DISCUSSION

Design of Mutant CD4D12. Most of the residues important for binding gp120 reside in the D1 domain (residues 1−99) of CD4 and lie between residues 25 and 64 (Figure 1A). D1 and D2 domains pack closely against each other with a large interfacial hydrophobic surface area (607 $Å^2$), and it has been shown previously that several mutations in the D1 domain of CD4 interfere with the gp120−CD4 interaction. Earlier we have reported the *E. coli* expression, purification, and

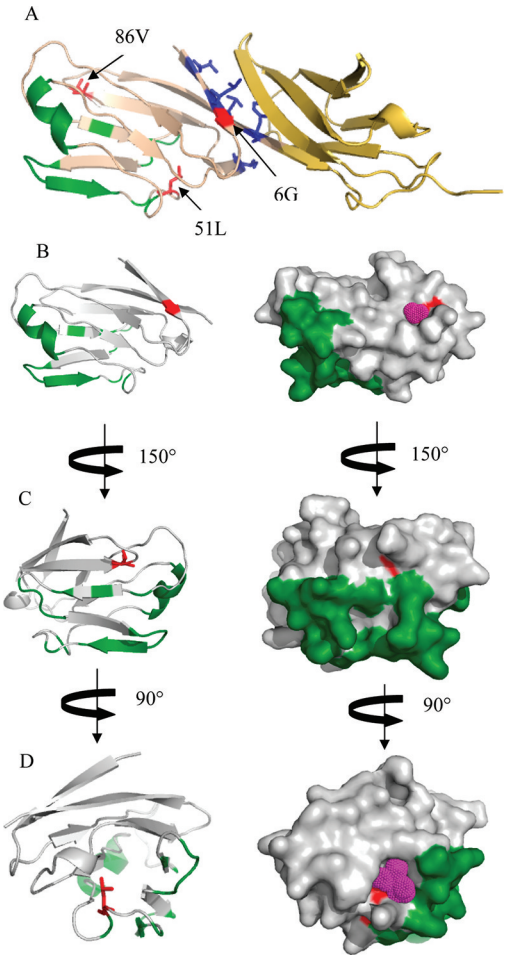

Figure 1. Locations of cavity filling and interface mutations in CD4D12. (A) Structure of CD4D12 (chain C of PDBID 1G9M). Domain D1 (residues 1−99) is shown in light pink, and domain D2 (residues 100−183) is shown in yellow-orange. The locations of the three cavity filling mutations G6A, L51I, and V86L are highlighted in red. The hydrophobic interface residues 3V, 5L, 76I, 96L, and 98F are highlighted in blue, and gp120 interacting residues of CD4 are highlighted in green. (B−D) Structure of D1 domain of CD4 shows residues mutated to fill the cavity in red and residues which interact with gp120 in green. A cartoon diagram is shown in the left panel, and a corresponding surface diagram is shown in the right panel. The orientation of D1 in (A) and (B) is identical. The residues highlighted are 6G, 86V, and 51L in (B), (C), and (D), respectively. The magenta spheres in (B) and (D) indicate the position of the nearby cavity detected by the program MC_CAVITY.

biophysical characterization of wt-CD4D12 and a derivative of CD4D1 with mutations at the D1:D2 interface.[12,13] Wt-CD4D12 could be refolded from inclusion bodies. However, the protein was prone to aggregation and amyloid fibril formation upon storage at 4 °C or upon thawing of frozen solutions.[13] To increase the stability of wt-CD4D12, in the present work the sequence of the protein was optimized using the program ROSETTADESIGN using a procedure similar to that of Dantas et al.[35] All sequence positions were allowed to vary with the constraint that only polar to polar/charged and nonpolar to nonpolar substitutions were allowed. It was observed that substitutions were consistently seen at three buried positions (G6, L51, and V86). We next used the previously described program MC_CAVITY[33] to examine if there were cavities in the neighborhood of the above residues in CD4D12. The program detected cavities near residues 6G and 51L (Figure 1B,D). Although no cavity was detected by the program near 86V, by visual inspection it was apparent that a small cavity was present (Figure 1C). Next, each of these three nonpolar residues were allowed to vary in identity to other nonpolar residues to fill the buried cavities, and the best substitution was selected on the basis of the calculated energy values and visual inspection. These mutations and energy calculations were done using the program ROSETTADESIGN (version 2.3.0). For each modeled residue at each position, four energy terms were calculated—Eatr = Lennard-Jones attractive energy, Erep = Lennard-Jones repulsive energy, Esolv = Lazaridis−Karplus solvation energy, Ehbond = energy of hydrogen bonding—and were summed up to get Etotal. Each of the energy terms are the difference between measured energies minus expected energies. Expected energies are derived by calculating the average energies of the same amino acid with a certain number of neighbors in a large set of proteins in the PDB (see http://www.rosettacommons.org/guide/Design). Hence, Etotal is not the energy difference between mutant and wild-type protein, but rather a measure of the energy of the given residue in CD4, relative to the average energy of the same residue in a similar environment, averaged over multiple protein structures in the PDB. In all the three positions the mutated nonpolar residue was chosen from the list by visual inspection of the modeled structure, subjected to the constraint that the chosen mutant had a value of Etotal less than 2 Rosetta energy units and a size increase of less than 3 methylene groups relative to the wild-type residue. The program ROSETTADESIGN tends to place amino acids with similar chemical properties near each other (see http://rosettadesign.med.unc.edu/documentation.php).This is primarily because polar residues can form hydrogen bonds to each other, and hydrophobics can pack without burial of hydrogen bonding groups. Sometimes polar groups are buried without a hydrogen bonding partner. The energy function has been parametrized to try and avoid this, but there is no filter that prevents it; hence, visual inspection is necessary. In case of positions 51 and 86, Met was not chosen even though it had low values of Etotal because it is a flexible side chain. The final cavity filling mutations incorporated individually into CD4D12 were G6A, V86L, and L51I, and calculated energy values are shown in Table S1.

Design of CD4D1a. Previously, a construct consisting of the D1 domain of CD4 that included residues 1−99 along with the following mutations at the D1:D2 interface was purified and biophysically characterized by us. The interface mutations were V3T, L5A, I76T, L96A, and F98A. The nonpolar residues at the interface was all mutated to Ala (to reduce the hydrophobicity) with the exception of I76, which was mutated to the polar threonine residue. No energy calculations were employed in this earlier study. This protein bound gp120 with 3-fold lower affinity compared to wt-CD4D12. The far-UV CD spectrum of the protein showed a peak with negative ellipticity at 205 nm and a fluorescence emission maximum of around 355 nm (with 280 nm excitation) and showed a broad peak in analytical gel filtration.[13] Besides, this protein was prone to degradation, even upon storage at −70 °C. All of these observations indicated that the earlier CD4D1 construct was substantially unfolded. To increase the structure and stability of the protein, the two cavity filling mutations G6A and V86L were introduced into CD4D1. Since the D1 and D2 domains of CD4 pack against each other

with a large hydrophobic interface (~600 Å^2), the absence of the D2 domain leads to the exposure of hydrophobic residues on the protein surface, leading to the aggregation of the protein. CD4D1 has a total accessible surface area (ASA) of 5878 Å^2, of which 607 Å^2 is involved in interaction with D2. This consists of five hydrophobic nonpolar residues (Val3, Leu5, Ile76, Leu96, Phe98) (Figure 1A) and four hydrophilic polar amino acids (Lys7, Lys8, Ser79, Gln94). Using the program ROSETTADESIGN, each hydrophobic residue in D1 having ΔASA (ΔASA = ASA in the absence of domain D2- ASA in presence of domain D2) value greater than 15 Å^2 was allowed to vary in identity to all polar residues separately. For each modeled residue at every single position, the total energy was calculated by summing up the four energy terms, as described above (Etotal = Eatr + Erep + Esolv + Ehbond). For the interface residue 5L the mutation with lysine was chosen based on the lowest energy substitution. In case of 98F, we avoided the introduction of another charged residue, since already one charged mutation had been introduced at 5L in the vicinity of 98F. Among the uncharged polar residues threonine was selected, as visual inspection showed a possible hydrogen bond with the backbone of Val97 and the value of Etotal for this substitution was less than 2 Rosetta energy units.

This construct with the four mutations listed above (L5K, G6A, V86L, F98T) is named CD4D1a to distinguish it from the partially unfolded CD4D1 construct described previously.[13]

Protein Purification and Gel Filtration. G6A-CD4D12, V86L-CD4D12, L51I-CD4D12, and CD4D1a were cloned in the pET28a(+) vector with an N-terminal His-tag and expressed in *E. coli* BL21(DE3) cells. Following cell growth and lysis, proteins were purified from resolubilized inclusion bodies using Ni-NTA affinity chromatography and refolded by dialysis against PBS. The yield was about 25 mg/L of culture for G6A-CD4D12, 20 mg/L of culture for V86L-CD4D12 and wt-CD4D12, and 10 mg/L of culture for CD4D1 and CD4D1a. L51I-CD4D12 was prone to degradation. Hence, it was not studied further. SDS-PAGE analysis confirmed that the proteins were at least 90% pure.

Gel-filtration chromatography was carried out for all mutants to assess their aggregation state. Both CD4D12 mutants and CD4D1a eluted as monomers under native conditions (PBS, pH 7.4) with sharp peaks (Figure 2) (data not shown for the CD4D12 mutants). This is in contrast to the CD4D1 construct reported previously. That was shown to elute as a broad peak under the same conditions due to the presence of significant amounts of both folded and unfolded species in rapid equilibrium with each other.[13] Therefore, the G6A and V86L mutations have improved the stability of the native state of the protein as intended.

Spectroscopic Characterization. The secondary structures of the mutants were analyzed by far-UV CD spectroscopy (Figure 3). The CD spectra of the two CD4D12 mutants were quite similar to the wt-CD4D12 protein with minima at 218 nm for the G6A and at 210 nm for the V86L mutant that is characteristic of β-sheet proteins. However, for G6A-CD4D12, the increase in positive ellipticity at 200 nm as well as a red shift of the negative ellipticity peak relative to wt-CD4D12 and V86L mutant is indicative of a higher secondary structure content for the G6A mutant, relative to wild-type and V86L mutant of CD4D12. CD4D1a also showed a well-defined secondary structure with a minimum at 225 nm. This is in contrast to the CD spectra reported for the earlier CD4D1

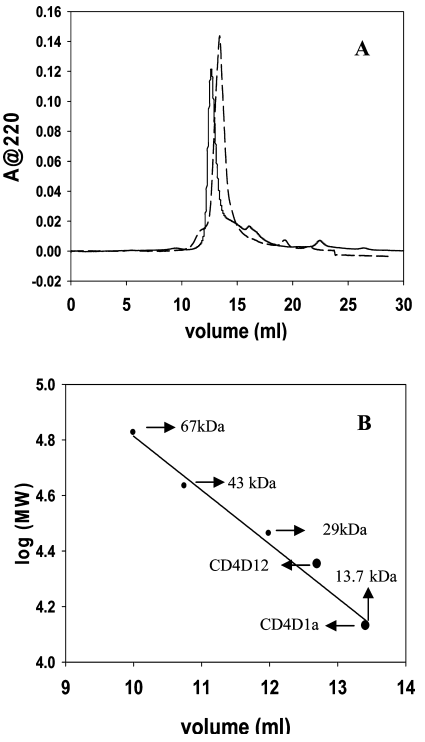

Figure 2. Gel-filtration analysis of CD4D12 and CD4D1a on an analytical Superdex 75 gel-filtration column in PBS at room temperature: (A) wt-CD4D12 (—) and CD4D1a (---). The absorbance at 220 nm is shown as a function of the elution volume. The plot shows that both proteins elute at the expected position for the respective monomer. CD4D12 mutants had identical elution profiles to wt. (B) Calibration curve using standard marker proteins albumin (67 kDa), ovalbumin (43 kDa), carbonic anhydrase (29 kDa), and ribonuclease A (13.7 kDa).

protein,[13] which had a minimum at 205 nm that is characteristic of proteins with short, irregular β strands.

The tertiary structure of the mutants was further analyzed by measuring the intrinsic fluorescence emission spectra of the proteins in native buffer and in the presence of 8 M urea (Figure 4). The native fluorescence emission spectra of the CD4D12 mutants showed an emission maximum at 340 nm, which is similar to the emission maximum of wt-CD4D12.[13] The presence of 8 M urea leads to a red shift to 358 nm and an increase in the fluorescence intensity. The red shift indicates exposure of tryptophan residues of CD4D12 to the solvent upon denaturation and the increase in intensity indicates that one or more of these tryptophan residues are quenched in the native structure. The native and 8 M urea fluorescence emission spectra of CD4D1a showed emission maxima at 348 and 360 nm, respectively, in contrast to CD4D1 which showed an emission maximum at 355 nm in the absence of denaturant.[13]

Thermal and Chemical Denaturation. The thermodynamic stabilities of the mutants were determined by thermal melts, monitored by following the ellipticities at 222 nm over a temperature range of 20−95 °C (Figure 5). Both CD4D12 mutants showed apparent two-state transitions with midpoints of the thermal transitions (T_m) at 76 °C for the G6A mutant and at 75 °C for the V86L mutant. This shows that both G6A-CD4D12 and V86L-CD4D12 mutants are more stable compared to wt-CD4D12 (T_m of 67 °C). It was also observed that while the G6A-CD4D12 mutant formed irreversible

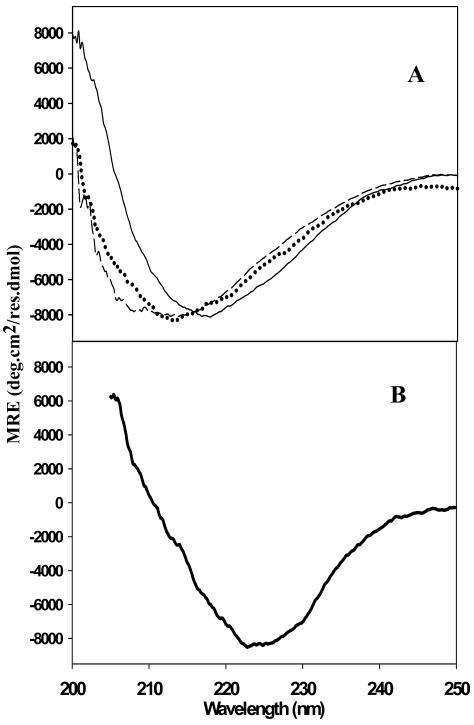

Figure 3. Far-UV CD spectra of (A) wt-CD4D12 (···), G6A-CD4D12 (—), and V86L-CD4D12 (---) and (B) CD4D1a. Spectra were obtained with 15 μM protein solution in PBS (pH 7.4), 298 K, with a 0.1 cm path-length cuvette.

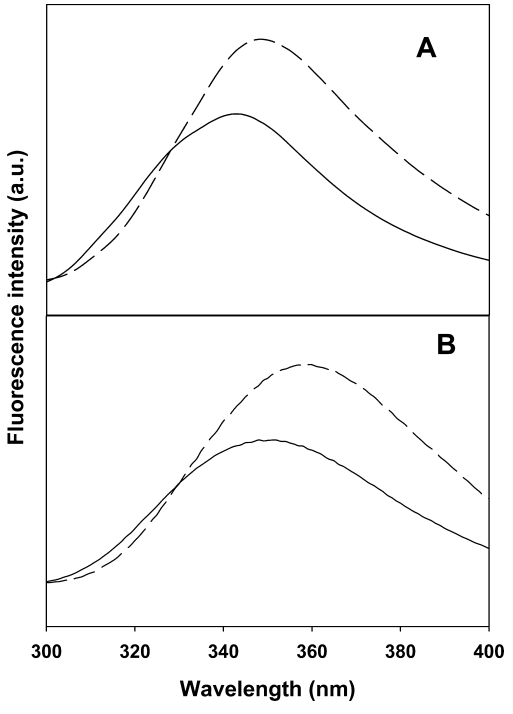

Figure 4. Fluorescence emission spectra for CD4D12 and CD4D1a. Protein samples were at a final concentration of 2 μM either in PBS (—) or in 8 M urea (---) at 25 °C and pH 7.4. Spectra were obtained with excitation at 280 nm and emission from 300 to 400 nm. (A) wt-CD4D12; (B) CD4D1a. CD4D12 mutants had identical spectra to wt.

aggregates at higher temperatures similar to wt-CD4D12, the V86L-CD4D12 mutant did not form aggregates, and its thermal

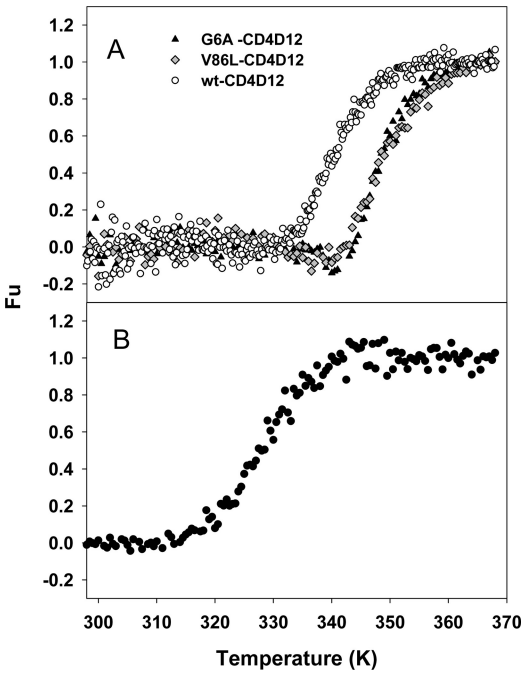

Figure 5. Thermal denaturation of (A) CD4D12 proteins and (B) CD4D1a in PBS (pH 7.4). The CD signal at 222 nm was recorded as a function of temperature. Data were converted to fraction unfolded (Fu) as described.[37] Protein concentration was 15 μM, time constant was 4 s, and the scan rate was 1 K/min.

melt was reversible. CD4D1a mutant showed a slightly broader thermal transition with a midpoint (T_m) of about 57 °C, indicating a stable but less cooperative transition compared to the CD4D12 proteins. CD4D1 did not show a clearly defined cooperative thermal transition (data not shown). Therefore, the G6A and V86L mutations appear to have improved the structure and stability of the CD4D1a construct compared to CD4D1.

The stabilities of all mutants were also monitored by denaturant-induced equilibrium unfolding studies at 25 °C by monitoring the intrinsic fluorescence emission in increasing concentrations of urea (Figure 6). The unfolding transitions for the CD4D12 mutants were broad and non-two-state, similar to that observed for wt-CD4D12. Hence, it was not possible to measure free energies of unfolding. The apparent midpoints of the transition are at 5.6, 5.4, and 5 M urea for G6A-CD4D12, V86L-CD4D12, and wt-CD4D12, respectively. Since clear unfolded baselines could not be obtained, the apparent midpoints were calculated assuming that the fluorescence signal at 8 M urea is entirely due to unfolded protein and that the unfolded baseline has a slope of zero. Therefore, it appears that the G6A and V86L mutations have led to increased stabilization of the protein. This agrees with the results from the CD-monitored thermal melts carried out for these mutants. CD4D1a also showed a broad unfolding transition with an apparent midpoint of transition at 5 M urea.

Proteolysis and Stability in Serum. Proteolytic digestion with trypsin was carried out to probe the stability of all the constructs. Figure 7A shows the digestion profile of wt-CD4D12, G6A-CD4D12, and V86L-CD4D12 by trypsin at 37 °C. In all cases, the protein was rapidly cleaved to give a proteolytically stable fragment of slightly lower (~1 kDa) molecular weight than the starting protein. This is likely to be

dx.doi.org/10.1021/bi200870r | Biochemistry 2011, 50, 7891–7900

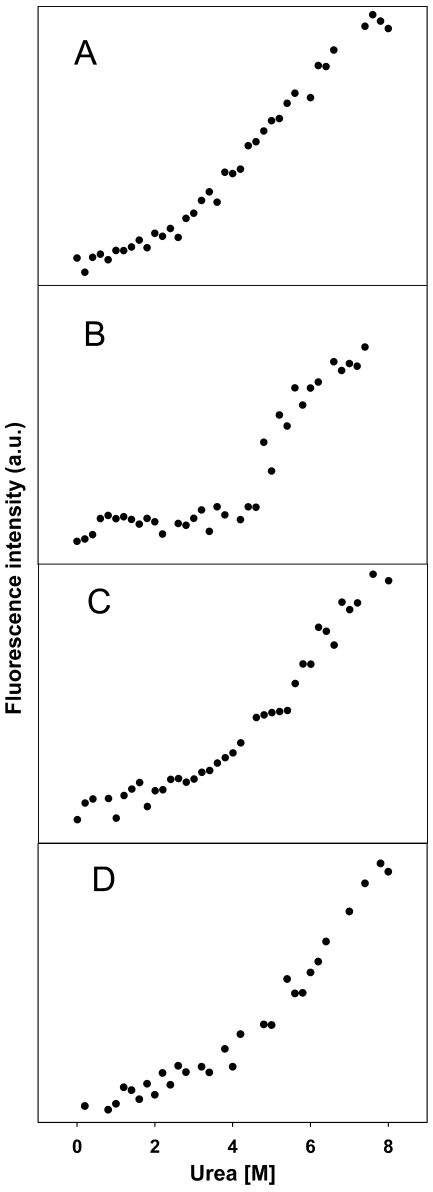

Figure 6. Urea denaturation, monitored by Trp fluorescence of CD4 derivatives at 25 °C, pH 7.4: (A) wt-CD4D12, (B) G6A-CD4D12, (C) V86L-CD4D12, (D) CD4D1a. Protein concentration was 2 μM. The intrinsic fluorescence signal was monitored as a function of urea concentration at 350 and 365 nm for CD4D12 and CD4D1 proteins, respectively.

due to cleavage at the N-terminal His-tag by the protease. Although there was no substantial difference in intensity of the low molecular weight band for wt-CD4D12, G6A-CD4D12, and V86L-CD4D12, from visual inspection G6A-CD4D12 seems to be slightly more resistant to proteolysis compared to the wild-type and the V86L mutant. Similarly, as described above, CD4D1a was also subjected to proteolysis by trypsin at 37 and 20 °C (Figure 7B). The protein was digested at 37 °C within 15 min but was relatively stable to cleavage at 20 °C. The stability of CD4D1a in serum was assessed by incubating the His-tagged protein in serum at 37 °C in the presence of Ni-NTA beads and then removing samples from the reaction mixture at different time points. The supernatant and the beads at the different time points were then analyzed by SDS-PAGE (Figure 7D). Most of the CD4D1a protein was bound to the

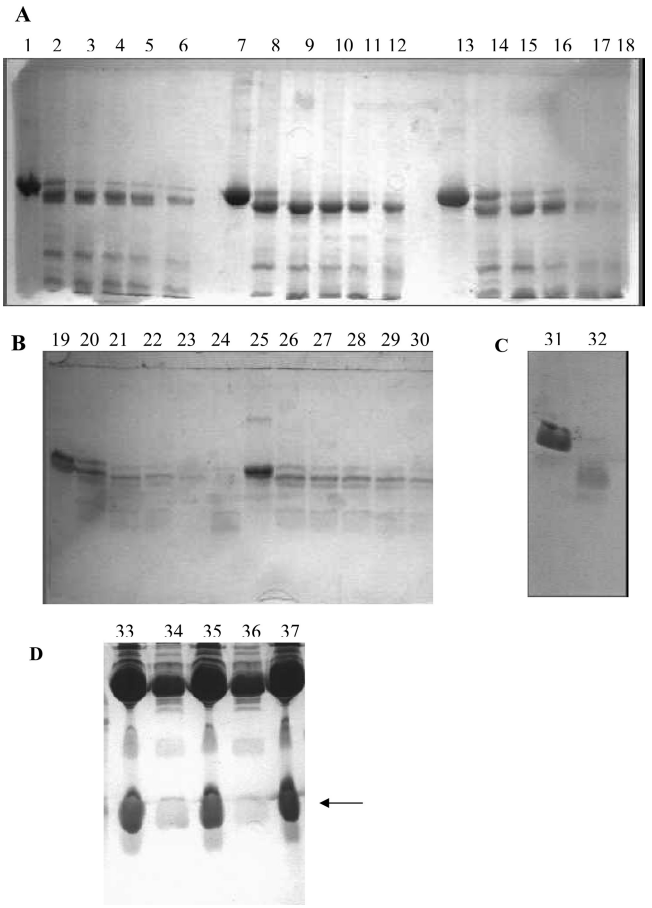

Figure 7. SDS-PAGE analysis of proteolytic digests of (A) CD4D12 derivatives, (B) CD4D1a, and (C) reduced carboxymethylated RNaseA (at pH 8.0) by trypsin. Lanes 1–6 in panel A indicate aliquots of the digestion mixture of wt-CD4D12 at time points 0 (undigested), 5, 15, 25, 40, and 60 min, respectively at 37 °C. Lanes 7–12 in panel A indicate aliquots of the digestion mixture of G6A-CD4D12 at time points 0 (undigested), 5, 15, 25, 40, and 60 min, respectively, at 37 °C, and lanes 13–18 contain aliquots of the digestion mixture of V86L-CD4D12 at time points 0 (undigested), 5, 15, 25, 40, and 60 min, respectively, at 37 °C. Lanes 19–24 in panel B indicate aliquots of the digestion mixture of CD4D1a at time points 0 (undigested), 5, 15, 25, 40, and 60 min, respectively, at 37 °C, and lanes 25–30 indicate aliquots of the digestion mixture of CD4D1a at time points 0 (undigested), 5, 15, 25, 40, and 60 min, respectively, at 20 °C. Lanes 31 and 32 contain digestion mixtures of reduced carboxymethylated RNaseA at time points 0 (undigested) and 5 min, respectively, at 20 °C. Proteolysis was stopped at the indicated time points by addition of formic acid at a final concentration of 0.1%. Samples were boiled with SDS-PAGE gel loading dye (final concentration 50 mM Tris-HCl containing 2% SDS, 0.1% bromophenol blue, and 100 mm DTT) prior to loading on the gel. Following electrophoresis, proteins were visualized by staining with Coomassie brilliant Blue R250. (D) SDS-PAGE analysis of CD4D1a after incubation in serum. 30 μg of His-tagged CD4D1a (in 100 μL) was incubated in 100 μL of serum at 37 °C in the presence of 20 μL of Ni-NTA beads, and 40 μL aliquots were removed from the reaction mixture at different time points. For every time point, the beads were spun down, and both the supernatant and beads were subjected to SDS-PAGE. Lanes 33, 35, and 37 indicate beads after 5 min, 1 h, and 8 h, respectively. Lanes 34 and 36 indicate supernatant after 5 min and 1 h, respectively. The gel shows that CD4D1a is stable in serum. The arrow indicates the position of CD4D1a.

dx.doi.org/10.1021/bi200870r | *Biochemistry* 2011, 50, 7891–7900

Ni-NTA beads even after 8 h of incubation, indicating that the protein is stable in serum. No further degradation was observed even after 24 h of incubation.

Binding Studies. The binding of the sCD4 and CD4D1 proteins to gp120 was determined *in vitro* using surface plasmon resonance (SPR) (Figure 8). The K_D calculated for

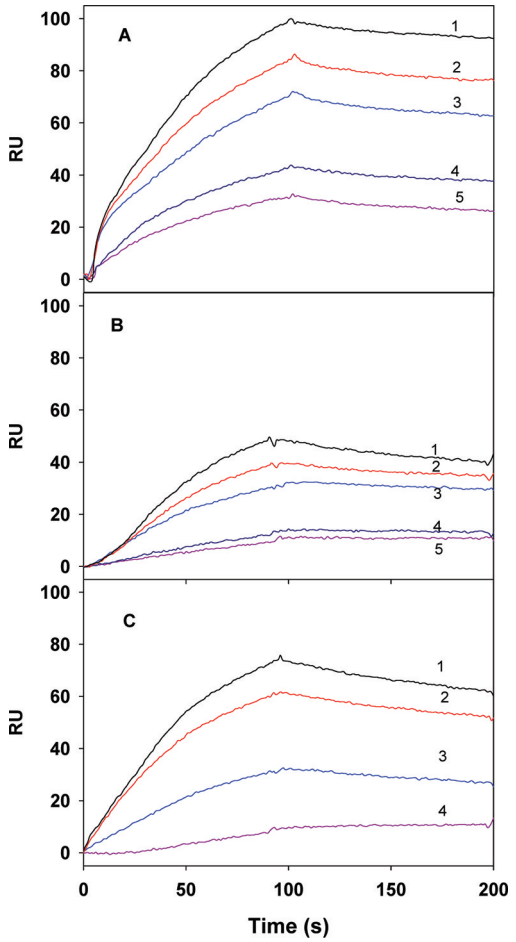

Figure 8. Sensorgram overlays for the binding of different concentrations of CD4 to surface immobilized gp120. (A) Commercial 4-domain CD4; (B) CD4D1; (C) CD4D1a. For (A) and (B), 1, 2, 3, 4, and 5 respectively indicate CD4 concentrations of 200, 150, 100, 50, and 25 nM, respectively. For (C) 1, 2, 3, and 4 respectively denote 150, 100, 50, and 25 nM concentrations of CD4D1a. Surface density 1000RU; buffer 10 mM HEPES (pH = 7.4), 150 mM NaCl, 3 mM EDTA, 0.005% P20, flow rate, 30 μL/min; temperature 298 K.

G6A-CD4D12 (K_D = 5.6 nM) and V86L-CD4D12 (K_D = 6.9 nM) are quite similar to wt-CD4D12 (K_D = 6 nM) and sCD4 (K_D = 12.8 nM). The K_D calculated for CD4D1a was 31 nM, which is similar to that of the CD4D1 protein (30 nM) (Table 1). This indicates that although the G6A and V86L mutations resulted in a better folded and more stable protein, this did not appear to have a substantial effect on gp120 binding. The CD4D1a protein has slightly higher k_{on} and k_{off} rates compared to CD4D1; however, the overall binding constant remains the same, and it was ~3-fold lower compared to soluble 4-domain CD4 (K_D = 12.8 nM).

Neutralization Studies. The ability of the CD4D12 and CD4D1a proteins to inhibit viral entry was studied. Since G6A-CD4D12 was the most stable of the CD4D12 proteins studied and had similar affinity for gp120 as wt-CD4D12, it was used in the neutralization studies. For the *in vitro* neutralization experiments, four subtype B viruses (SF162, BAL, JRCSF, and NL4-3) and one subtype C virus (98IN022) were used. IC_{50} values obtained are shown in Table 2 and compared with published values from the literature that were obtained with soluble 4-domain CD4. The data show that both CD4D1a and G6A-CD4D12 have IC_{50} values similar to those of commercially available soluble CD4. Deletion of the D2 domain, therefore does not appear to affect the ability of soluble CD4 to neutralize HIV-1.

Table 1. SPR Determined Kinetic Parameters for Binding of sCD4, wt-CD4D12, Mutant CD4D12, CD4D1, and CD4D1a to Surface Immobilized Full Length gp120

ligand	k_{on} ($M^{-1}s^{-1}$)	k_{off} (s^{-1})	K_D (nM)
sCD4	7.2×10^4	9.2×10^{-4}	12.8
wt-CD4D12	4.3×10^4	2.6×10^{-4}	6
G6A-CD4D12	1.7×10^5	9.6×10^{-4}	5.6
V86L-CD4D12	5.8×10^4	4×10^{-4}	6.9
CD4D1	3.9×10^4	1.17×10^{-3}	30
CD4D1a	5.4×10^4	1.7×10^{-3}	31

Table 2. Neutralization Titers (IC_{50} in μg/mL) of G6A-CD4D12, CD4D1a, and Soluble CD4 for Various HIV-1 Isolates

	IC_{50} (μg/mL)		
virus	CD4D1a	soluble CD4	G6A-CD4D12
SF162	0.13	0.05[a]	0.19
BAL	0.10	0.14[b,f]	0.11
JRCSF	48.6	~35[c]	88.5
NL4-3	0.08	0.1[d]	0.08
98IN022	1.5	–[e]	1.8
aMLV	>100	>100	>100

[a]IC_{50} value obtained from ref 40. [b]IC_{50} value for obtained from ref 14. [c]IC_{50} value for obtained from ref 8. [d]IC_{50} value obtained from ref 41. [e]Not done. [f]IC_{50} value reported for N-terminal 2-domain CD4.

CONCLUSIONS

Different derivatives of wt-CD4D12 and CD4D1[42] have been constructed and characterized. Two cavity filling mutations in wt-CD4D12 (G6A and V86L) have been introduced. Both proteins are monomeric, folded, and have increased stability and yield relative to wt-CD4D12. CD4 residues interacting with gp120 are all in the D1 domain. To generate a stable smaller fragment of CD4, the two stabilizing cavity filling mutations identified in CD4D12 as well as two surface mutations were introduced into domain D1 to minimize the aggregation and degradation of the protein. Biophysical characterization has shown that this mutant protein (CD4D1a) is better folded and more stable compared to CD4D1 described previously,[13] but it bound gp120 with similar affinity to the earlier molecule. Both CD4D1a and G6A-CD4D12 were able to neutralize different viruses, with similar IC_{50}s as 4-domain soluble CD4. These proteins are a useful starting point for the design of other, more complex viral entry inhibitors. Furthermore, the present studies show that cavity filling mutations are a viable approach to stabilize domains of the IgG fold and therefore can potentially

be used to stabilize monoclonal antibodies and other members of this important fold.

■ ASSOCIATED CONTENT

Supporting Information

Energy values of cavity filling mutations in CD4D12 (Table S1) and interface mutations of CD4D1a (Table S2) using the program ROSETTADESIGN. This material is available free of charge via the Internet at http://pubs.acs.org.

■ AUTHOR INFORMATION

Corresponding Author

*E-mail schief@u.washington.edu (W.R.S.); Tel 91-80-22932612, Fax 91-80-23600535, e-mail varadar@mbu.iisc.ernet.in (R.V.).

Author Contributions

Authors P.S. and B.B have contributed equally to this work.

Funding

This work was supported by grants from the Department of Biotechnology, Government of India, and International AIDS Vaccine Initiative to R.V. P.S. and S.B. are recipients of fellowships from Council of Scientific and Industrial Research, Government of India.

■ ACKNOWLEDGMENTS

We thank Siddharth Patel and Bharat V. Adkar for help with cavity calculations.

■ ABBREVIATIONS

CD4D12, first two domains of CD4; wt-CD4D12, wild-type CD4D12; sCD4, soluble 4-domain CD4; hCD4, human CD4; CD4D1, previously engineered first domain of CD4; CD4D1a, currently engineered CD4D1; env, HIV-1 envelope glycoprotein; $CD4_i$, CD4-induced epitopes of gp120; ASA, accessible surface area; IPTG, isopropyl-β-thiogalactopyranoside; PBS, phosphate buffered saline; GdnCl, guanidine hydrochloride; RU, resonance units; CD, circular dichroism; MRE, mean residue ellipticity; rcam-RNaseA, reduced carboxymethylated RNaseA; SPR, surface plasmon resonance.

■ REFERENCES

(1) Dalgleish, A. G., Beverley, P. C., Clapham, P. R., Crawford, D. H., Greaves, M. F., and Weiss, R. A. (1984) The CD4 (T4) antigen is an essential component of the receptor for the AIDS retrovirus. *Nature 312*, 763−767.

(2) Lasky, L. A., Nakamura, G., Smith, D. H., Fennie, C., Shimasaki, C., Patzer, E., Berman, P., Gregory, T., and Capon, D. J. (1987) Delineation of a region of the human immunodeficiency virus type 1 gp120 glycoprotein critical for interaction with the CD4 receptor. *Cell 50*, 975−985.

(3) Berger, E. A., Fuerst, T. R., and Moss, B. (1988) A soluble recombinant polypeptide comprising the amino-terminal half of the extracellular region of the CD4 molecule contains an active binding site for human immunodeficiency virus. *Proc. Natl. Acad. Sci. U. S. A. 85*, 2357−2361.

(4) Hussey, R. E., Richardson, N. E., Kowalski, M., Brown, N. R., Chang, H. C., Siliciano, R. F., Dorfman, T., Walker, B., Sodroski, J., and Reinherz, E. L. (1988) A soluble CD4 protein selectively inhibits HIV replication and syncytium formation. *Nature 331*, 78−81.

(5) Fisher, R. A., Bertonis, J. M., Meier, W., Johnson, V. A., Costopoulos, D. S., Liu, T., Tizard, R., Walker, B. D., Hirsch, M. S., Schooley, R. T., et al. (1988) HIV infection is blocked in vitro by recombinant soluble CD4. *Nature 331*, 76−78.

(6) Traunecker, A., Luke, W., and Karjalainen, K. (1988) Soluble CD4 molecules neutralize human immunodeficiency virus type 1. *Nature 331*, 84−86.

(7) Deen, K. C., McDougal, J. S., Inacker, R., Folena-Wasserman, G., Arthos, J., Rosenberg, J., Maddon, P. J., Axel, R., and Sweet, R. W. (1988) A soluble form of CD4 (T4) protein inhibits AIDS virus infection. *Nature 331*, 82−84.

(8) Daar, E. S., Li, X. L., Moudgil, T., and Ho, D. D. (1990) High concentrations of recombinant soluble CD4 are required to neutralize primary human immunodeficiency virus type 1 isolates. *Proc. Natl. Acad. Sci. U. S. A. 87*, 6574−6578.

(9) Davis, C. B., Boyle, K. E., Urbanski, J. J., Paradysz, R. T., and Fong, K. L. (1992) Disposition of metabolically labeled recombinant soluble CD4 (sT4) in male Sprague-Dawley rats following intravenous and subcutaneous administration. *Drug Metab. Dispos. 20*, 695−705.

(10) Cerutti, N., Mendelow, B. V., Napier, G. B., Papathanasopoulos, M. A., Killick, M., Khati, M., Stevens, W., and Capovilla, A. (2010) Stabilization of HIV-1 gp120-CD4 receptor complex through targeted interchain disulfide exchange. *J. Biol. Chem. 285*, 25743−25752.

(11) Fouts, T., Godfrey, K., Bobb, K., Montefiori, D., Hanson, C. V., Kalyanaraman, V. S., DeVico, A., and Pal, R. (2002) Crosslinked HIV-1 envelope-CD4 receptor complexes elicit broadly cross-reactive neutralizing antibodies in rhesus macaques. *Proc. Natl. Acad. Sci. U. S. A. 99*, 11842−11847.

(12) Varadarajan, R., Sharma, D., Chakraborty, K., Patel, M., Citron, M., Sinha, P., Yadav, R., Rashid, U., Kennedy, S., Eckert, D., Geleziunas, R., Bramhill, D., Schleif, W., Liang, X., and Shiver, J. (2005) Characterization of gp120 and its single-chain derivatives, gp120-CD4D12 and gp120-M9: implications for targeting the CD4i epitope in human immunodeficiency virus vaccine design. *J. Virol. 79*, 1713−1723.

(13) Sharma, D., Balamurali, M. M., Chakraborty, K., Kumaran, S., Jeganathan, S., Rashid, U., Ingallinella, P., and Varadarajan, R. (2005) Protein minimization of the gp120 binding region of human CD4. *Biochemistry 44*, 16192−16202.

(14) Wilkinson, R. A., Piscitelli, C., Teintze, M., Cavacini, L. A., Posner, M. R., and Lawrence, C. M. (2005) Structure of the Fab fragment of F105, a broadly reactive anti-human immunodeficiency virus (HIV) antibody that recognizes the CD4 binding site of HIV type 1 gp120. *J. Virol. 79*, 13060−13069.

(15) Richards, F. M. (1974) The interpretation of protein structures: total volume, group volume distributions and packing density. *J. Mol. Biol. 82*, 1−14.

(16) Chothia, C. (1975) Structural invariants in protein folding. *Nature 254*, 304−308.

(17) Kellis, J. T. Jr., Nyberg, K., Sali, D., and Fersht, A. R. (1988) Contribution of hydrophobic interactions to protein stability. *Nature 333*, 784−786.

(18) Kellis, J.T. Jr., Nyberg, K., and Fersht, A. R. (1989) Energetics of complementary side-chain packing in a protein hydrophobic core. *Biochemistry 28*, 4914−4922.

(19) Varadarajan, R., and Richards, F. M. (1992) Crystallographic structures of ribonuclease S variants with nonpolar substitution at position 13: packing and cavities. *Biochemistry 31*, 12315−12327.

(20) Jackson, S. E., Moracci, M., elMasry, N., Johnson, C. M., and Fersht, A. R. (1993) Effect of cavity-creating mutations in the hydrophobic core of chymotrypsin inhibitor 2. *Biochemistry 32*, 11259−11269.

(21) Ratnaparkhi, G. S., and Varadarajan, R. (2000) Thermodynamic and structural studies of cavity formation in proteins suggest that loss of packing interactions rather than the hydrophobic effect dominates the observed energetics. *Biochemistry 39*, 12365−12374.

(22) Karpusas, M., Baase, W. A., Matsumura, M., and Matthews, B. W. (1989) Hydrophobic packing in T4 lysozyme probed by cavity-filling mutants. *Proc. Natl. Acad. Sci. U. S. A. 86*, 8237−8241.

(23) Ohmura, T., Ueda, T., Ootsuka, K., Saito, M., and Imoto, T. (2001) Stabilization of hen egg white lysozyme by a cavity-filling mutation. *Protein Sci. 10*, 313−320.

(24) Yoshida, Y., Ohkuri, T., Kino, S., Ueda, T., and Imoto, T. (2005) Elucidation of the relationship between enzyme activity and internal motion using a lysozyme stabilized by cavity-filling mutations. *Cell. Mol. Life Sci. 62*, 1047−1055.

(25) Eijsink, V. G., Dijkstra, B. W., Vriend, G., van der Zee, J. R., Veltman, O. R., van der Vinne, B., van den Burg, B., Kempe, S., and Venema, G. (1992) The effect of cavity-filling mutations on the thermostability of Bacillus stearothermophilus neutral protease. *Protein Eng. 5*, 421−426.

(26) Ishikawa, K., Nakamura, H., Morikawa, K., and Kanaya, S. (1993) Stabilization of Escherichia coli ribonuclease HI by cavity-filling mutations within a hydrophobic core. *Biochemistry 32*, 6171−6178.

(27) Morii, H., Uedaira, H., Ogata, K., Ishii, S., and Sarai, A. (1999) Shape and energetics of a cavity in c-Myb probed by natural and non-natural amino acid mutations. *J. Mol. Biol. 292*, 909−920.

(28) Lassalle, M. W., Yamada, H., Morii, H., Ogata, K., Sarai, A., and Akasaka, K. (2001) Filling a cavity dramatically increases pressure stability of the c-Myb R2 subdomain. *Proteins 45*, 96−101.

(29) Kono, H., Saito, M., and Sarai, A. (2000) Stability analysis for the cavity-filling mutations of the Myb DNA-binding domain utilizing free-energy calculations. *Proteins 38*, 197−209.

(30) Lee, C., Park, S. H., Lee, M. Y., and Yu, M. H. (2000) Regulation of protein function by native metastability. *Proc. Natl. Acad. Sci. U. S. A. 97*, 7727−7731.

(31) Sengupta, T., Tsutsui, Y., and Wintrode, P. L. (2009) Local and global effects of a cavity filling mutation in a metastable serpin. *Biochemistry 48*, 8233−8240.

(32) Kuhlman, B., Dantas, G., Ireton, G. C., Varani, G., Stoddard, B. L., and Baker, D. (2003) Design of a novel globular protein fold with atomic-level accuracy. *Science 302*, 1364−1368.

(33) Chakravarty, S., Bhinge, A., and Varadarajan, R. (2002) A procedure for detection and quantitation of cavity volumes proteins. Application to measure the strength of the hydrophobic driving force in protein folding. *J. Biol. Chem. 277*, 31345−31353.

(34) Murzin, A. G., Brenner, S. E., Hubbard, T., and Chothia, C. (1995) SCOP: a structural classification of proteins database for the investigation of sequences and structures. *J. Mol. Biol. 247*, 536−540.

(35) Dantas, G., Kuhlman, B., Callender, D., Wong, M., and Baker, D. (2003) A large scale test of computational protein design: folding and stability of nine completely redesigned globular proteins. *J. Mol. Biol. 332*, 449−460.

(36) Pace, C. N., Vajdos, F., Fee, L., Grimsley, G., and Gray, T. (1995) How to measure and predict the molar absorption coefficient of a protein. *Protein Sci. 4*, 2411−2423.

(37) Beena, K., Udgaonkar, J. B., and Varadarajan, R. (2004) Effect of signal peptide on the stability and folding kinetics of maltose binding protein. *Biochemistry 43*, 3608−3619.

(38) Richman, D.D., Wrin, T., Little, S. J., and Petropoulos, C. J. (2003) Rapid evolution of the neutralizing antibody response to HIV type 1 infection. *Proc. Natl. Acad. Sci. U. S. A. 100*, 4144−4149.

(39) Zolla-Pazner, S., Cohen, S., Pinter, A., Krachmarov, C., Wrin, T., Wang, S., and Lu, S. (2009) Cross-clade neutralizing antibodies against HIV-1 induced in rabbits by focusing the immune response on a neutralizing epitope. *Virology 392*, 82−93.

(40) Li, M., Gao, F., Mascola, J. R., Stamatatos, L., Polonis, V. R., Koutsoukos, M., Voss, G., Goepfert, P., Gilbert, P., Greene, K. M., Bilska, M., Kothe, D. L., Salazar-Gonzalez, J. F., Wei, X., Decker, J. M., Hahn, B. H., and Montefiori, D. C. (2005) Human immunodeficiency virus type 1 env clones from acute and early subtype B infections for standardized assessments of vaccine-elicited neutralizing antibodies. *J. Virol. 79*, 10108−10125.

(41) Huang, C. C., Stricher, F., Martin, L., Decker, J. M., Majeed, S., Barthe, P., Hendrickson, W. A., Robinson, J., Roumestand, C., Sodroski, J., Wyatt, R., Shaw, G. M., Vita, C., and Kwong, P. D. (2005) Scorpion-toxin mimics of CD4 in complex with human immunodeficiency virus gp120 crystal structures, molecular mimicry, and neutralization breadth. *Structure 13*, 755−768.

(42) Chen, W., Feng, Y., Gong, R., Zhu, Z., Wang, Y., Zhao, Q., and Dimitrov, D. S. (2011) Engineered single human CD4 domains as potent HIV-1 inhibitors and components of vaccine immunogens. *J. Virol.*, in press.

NOTE ADDED IN PROOF

While this paper was under review, another paper (42) reported an alternative design for CD4D1 using phage display.